

High Power 980 nm Ridge Waveguide Semiconductor Laser Diode

Liu Bin^{1,2} Liu Yuanyuan³

¹*Collaborative Innovation Center of Judicial Civilization, Beijing 100088, China;*

²*Key Laboratory of Evidence Science, China University of Political Science and Law, Ministry of Education, Beijing 100088, China;*

³*Institute of Semiconductors, Chinese Academy of Sciences, Beijing 100083, China.*

Abstract The design and fabrication of high power 980 nm ridge waveguide semiconductor laser diodes are described. To reduce the optical power density on facets, the broad-waveguide structure is designed. The 500 mW kink-free laser diodes is obtained by standard ridge waveguide laser diode process techniques, and the catastrophic optical damage (COD) level of the LDs is 560 mW.

Key words lasers; 980 nm semiconductor laser diodes; reliability; broad-waveguide; catastrophic optical damage

OCIS codes 140.5960; 140.3460

980 nm 高功率脊型波导半导体激光器

刘斌^{1,2} 刘媛媛³

¹司法文明协同创新中心, 北京 100088

²证据科学教育部重点实验室, 中国政法大学, 北京 100088

³中国科学院半导体研究所, 北京 100083

摘要 介绍了高功率 980 nm 脊型波导半导体激光器的设计及制造。为了减少腔面处的光功率密度, 设计了宽波导结构。利用常规工艺获得了最大 500 mW 输出的器件, 同时灾变光学损伤阈值达到了 560 mW。

关键词 激光器; 980 nm 半导体激光器; 可靠性; 宽波导; 灾变性光学损伤

中图分类号 TN958

文献标识码 A

doi: 10.3788/LOP52.091404

1 Introduction

Erbium-doped fiber amplifiers (EDFAs) are the key devices of dense wavelength-division multiplexing (DWDM) systems. The 980 nm pump laser diodes are identified to be practical pump sources for EDFAs^[1-2]. High power and highly reliable laser devices are in high demand in applications. A lot of studies are focused on improving the reliability of the 980 nm laser diodes^[3-6]. The degradation and catastrophic optical damage (COD) of facets are the main causes affecting the reliability of 980 nm laser diodes.

There are some techniques to improve the reliability of the 980 nm laser diodes: 1) Reduce the surface non-radiative recombination velocity by cleaving the wafer into bars in ultrahigh vacuum and to evaporate an appropriate passivation layer on the facets, or passivating the surface with ZnSe to replace the non-stable oxide by a more stable compound^[7]; 2) Decrease the initial light absorption at the facets. One possible method is using non-absorption windows to regrow high gap material near the facets^[8]. Another method is using quantum well disordering through ion implantation^[9]; 3) Reduce the leakage current to facets. The leakage current reduction technique is relatively simple and effective^[10].

收稿日期: 2015-03-10; 收到修改稿日期: 2015-03-01; 网络出版日期: 2015-08-12

基金项目: 北京市教育委员会共建项目、中国政法大学青年教师创新团队资助项目、证据科学教育部重点实验室(中国政法大学)开放基金(2011KFKT04, 2012KFKT08)

作者简介: 刘斌(1970—), 男, 博士, 副教授, 主要从事光电子技术与法庭科学方面的研究。E-mail: rays_liu@126.com

2 Design and fabrication

To reduce the power density on the facets, broad-waveguide structure is designed. Figure 1 (a) shows the schematic diagram of the refractive index (A), the calculated results according to the transverse near-field distribution (B), and the vertical far-field pattern [Fig1.(b)] for the broad-waveguide structure. The theoretical vertical far-field angle is 28° [full width at half maximum (FWHM)].

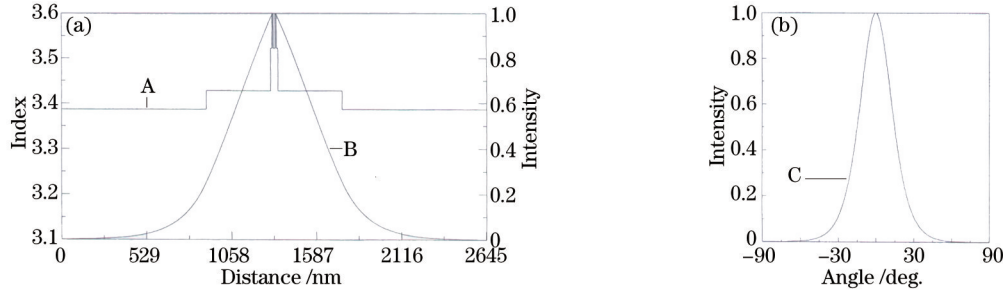


Fig.1 (a) Diagram of refractive index (A), and calculated results of transverse near-field distribution (B);
(b) vertical far-field pattern (C)

Epitaxial layers are grown by low-pressure metal-organic chemical vapor deposition (LP-MOCVD) on the (100) oriented Si-doped GaAs substrate with concentration of $1 \times 10^{18} \sim 3 \times 10^{18} \text{ cm}^{-3}$ in the Aixtron A200 system. The layer sequence is illustrated in Table 1, a n-GaAs buffer layer (0.3 μm , Si doped concentration of $1 \times 10^{18} \text{ cm}^{-3}$), a n- $\text{Al}_{0.23}\text{Ga}_{0.77}\text{As}$ cladding layer (900 nm, Si doped concentration of $1 \times 10^{18} \text{ cm}^{-3}$), a $\text{Al}_{0.16}\text{Ga}_{0.84}\text{As}$ waveguide layer (400 nm, doped partly), $\text{In}_{0.2}\text{Ga}_{0.8}\text{As}$ quantum well (7 nm), GaAs barrier layer (12 nm), $\text{In}_{0.2}\text{Ga}_{0.8}\text{As}$ quantum well (7 nm), GaAs barrier layer (10 nm), a $\text{Al}_{0.16}\text{Ga}_{0.84}\text{As}$ waveguide layer (400 nm, doped partly), P- $\text{Al}_{0.23}\text{Ga}_{0.77}\text{As}$ cladding layer (30 nm, Zn doped concentration of $6 \times 10^{17} \text{ cm}^{-3}$), 5 nm P-InGaAsP ($E_g = 1.61 \text{ eV}$) etch stop layer (Zn doped concentration of $6 \times 10^{17} \sim 2 \times 10^{18} \text{ cm}^{-3}$), P- $\text{Al}_{0.23}\text{Ga}_{0.77}\text{As}$ cladding layer (800 nm, Zn doped concentration of $2 \times 10^{18} \text{ cm}^{-3}$), P-GaAs top layer (200 nm, Zn doped concentration of $2 \times 10^{18} \sim 1 \times 10^{19} \text{ cm}^{-3}$), P⁺-GaAs cap layer (20 nm, Zn doped concentration of $1 \times 10^{19} \sim 1 \times 10^{20} \text{ cm}^{-3}$).

Table 1 Epitaxial layer sequence

Layer number	Material	Thickness	Note
13	P ⁺ -GaAs cap	20 nm	Zn: $1 \times 10^{19} \sim 1 \times 10^{20} \text{ cm}^{-3}$
12	P-GaAs top layer	200 nm	Zn: $2 \times 10^{18} \sim 1 \times 10^{19} \text{ cm}^{-3}$
11	P- $\text{Al}_{0.23}\text{Ga}_{0.77}\text{As}$ cladding	800 nm	Zn: $2 \times 10^{18} \text{ cm}^{-3}$
10	P-InGaAsP	5 nm	Zn: $6 \times 10^{17} \sim 2 \times 10^{18} \text{ cm}^{-3}$
9	P- $\text{Al}_{0.23}\text{Ga}_{0.77}\text{As}$ cladding	30 nm	Zn: $6 \times 10^{17} \text{ cm}^{-3}$
8	$\text{Al}_{0.16}\text{Ga}_{0.84}\text{As}$ waveguide	400 nm	doped partly
7	GaAs barrier layer	10 nm	
6	$\text{In}_{0.2}\text{Ga}_{0.8}\text{As}$ quantum well	7 nm	
5	GaAs barrier	12 nm	
4	$\text{In}_{0.2}\text{Ga}_{0.8}\text{As}$ quantum well	7 nm	
3	$\text{Al}_{0.16}\text{Ga}_{0.84}\text{As}$ waveguide	400 nm	doped partly
2	n- $\text{Al}_{0.23}\text{Ga}_{0.77}\text{As}$ cladding	900 nm	Si: $1 \times 10^{18} \text{ cm}^{-3}$
1	n-GaAs buffer	0.3 μm	Si: $1 \times 10^{18} \text{ cm}^{-3}$

After growth, the 4- μm -wide ridge waveguide LDs are fabricated by a standard 980 nm ridge waveguide laser diodes process. Low-reflection ($R_l=6\%$) and high-reflection ($R_h=95\%$) coating are formed on the front and the rear facets by electron cyclotron resonance-plasma chemical vapor deposition (ECR-PCVD). The cavity length of the laser diodes is 900 μm .

3 Results and discussion

Laser diodes are bonded on copper heat sink with p-side down configuration using indium solder. The experiment is carried out under the continuous-wave (CW) operation condition with room temperature of 23°C . The maximum 500 mW kink-free output is obtained at a driving current of 620 mA.

The COD level is 560 mW, the threshold current is 40 mA and the voltage of operation is 1.75 V for the output of 500 mW. The slop efficiency is 0.86 W/A. The wallplug efficiency is 46.3%. The series resistance is 0.56 W, and the vertical far-field divergence angle of FWHM is 30° , which is in good agreement with the theoretical analysis. Figure 2 shows the typical continuous-wave light output versus current ($P-I$) characteristics and COD profiles of the laser diodes.

A $\text{Al}_{0.16}\text{Ga}_{0.84}\text{As}$ waveguide layer (400 nm, doped partly) is the restrictions on both sides of the quantum well layer beam waveguide layer. The total width is about 800nm, which is much larger than the normal width of narrow waveguide layer (100~200 nm). This will reduce the cavity surface optical density, and accordingly help improve its reliability.

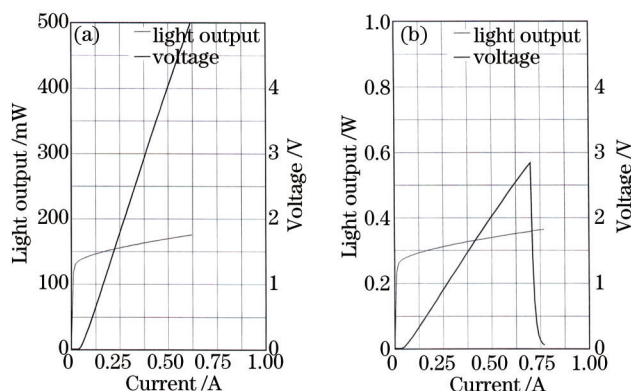


Fig.2 Typical CW $P-I$ characteristics and COD profile of LDs

4 Conclusions

To reduce the optical power density on facets, the broad-waveguide structure is designed to produce high power ridge waveguide laser diodes emitting at 980 nm. The maximum 500 mW kink-free output power is obtained at a driving current of 620 mA, and the COD level is 560 mW. The threshold current is 40 mA. The voltage of operation is 1.75 V for the output of 500 mW. The slop efficiency is 0.86 W/A. The wallplug efficiency is 46.3%. The series resistance is 0.56 W, and the vertical far-field divergence angle of FWHM is 30° , which is in good agreement with the theoretical analysis.

References

- 1 B Pedersen, B A Thompson, S Zemon, *et al.*. Power requirements for Erbium-doped fiber amplifiers pumped in 800, 980, and 1480 nm bands[J]. IEEE Photon Techno Lett, 1992, 4(1): 46-49.
- 2 E Desurvire. Spectral noise figure of Er^{3+} -doped fiber amplifiers[J]. IEEE Photon Techno Lett, 1990, 2(3): 208.
- 3 M Fukuda, M Okayasu, J Temmyo, *et al.*. Degradation behavior of 0.98- μm strained quantum well InGaAs/AlGaAs lasers under high-power operation[J]. IEEE J Quantum Electron, 1994, 30(2): 471-476.
- 4 A Moser, A Oosenbrug, E E Latta, *et al.*. High-power operation of strained InGaAs/AlGaAs single quantum well lasers[J]. Appl Phys Lett, 1991, 59(21): 2642-2644.
- 5 M Okayasu, M Fukuda, T Takeshita, *et al.*. Facet oxidation of InGaAs/GaAs strained quantum-well lasers[J]. J Appl Phys, 1991, 69(12): 8346-8351.
- 6 Chong Feng, Wang Jun, Xiong Cong, *et al.*. An asymmetric broad waveguide structure for a 0.98- μm high-conversion-efficiency diode laser[J]. Journal of Semiconductors, 2009, 30(6): 64-67.
- 7 A V Syrbu, V P Yakovlev, G I Suruceanu, *et al.*. ZnSe-facet-passivated InGaAs/InGaAsP/InGaP diode lasers of high CW power and 'wallplug' efficiency[J]. Electron Lett, 1996, 32(4): 352-353.
- 8 J E Ungau, N S K Kwong, S W Oh, *et al.*. High power 980 nm nonabsorbing facet lasers[J]. Electron Lett, 1994, 30: 1766-1767.
- 9 R L Thornton, R D Burnham, T L Paoli. Highly efficient multiple emitter index guided array lasers fabricated by silicon impurity induced disordering[J]. Appl Phys Lett, 1986, 48(1): 7-9.
- 10 M Sagawa, K Hiramoto, T Toyonaka, *et al.*. High power COD-free operation of 0.98 μm InGaAs/GaAs/InGaP lasers with non-injection regions near the facets[J]. Electron Lett, 1994, 30(17): 1410-1411.